Chemosphere 178 (2017) 42–50

Contents lists available at ScienceDirect

Chemosphere

journal homepage: www.elsevier.com/locate/chemosphere

Concentrations and isotope ratios of mercury in sediments from shelf and continental slope at Campos Basin near Rio de Janeiro, Brazil

Beatriz Ferreira Araujo [a, *], Holger Hintelmann [b], Brian Dimock [b], Marcelo Gomes Almeida [a], Carlos Eduardo Rezende [a]

[a] Universidade Estadual do Norte Fluminense, Centro de Biociências e Biotecnologia, Laboratório de Ciências Ambientais, Av. Alberto Lamego, 2000, Horto, CEP: 28013-602, Campos dos Goytacazes, RJ, Brazil
[b] Trent University, Water Quality Centre, 1600 West Bank Drive, Peterborough, ON, Canada

HIGHLIGHTS

- Riverine delivery of Hg could be an important source of Hg input to continental shelf.
- Hg and MMHg concentrations in CB sediments are comparable to background levels.
- Hg isotope ratios are an important tool to differentiate sources and processes of Hg.

ARTICLE INFO

Article history:
Received 11 July 2016
Received in revised form
19 February 2017
Accepted 12 March 2017

Handling Editor: Martine Leermakers

Keywords:
Mercury isotopes
Monomethylmercury
Campos Basin
Continental shelf

ABSTRACT

Mercury (Hg) may originate from both anthropogenic and natural sources. The measurement of spatial and temporal variations of Hg isotope ratios in sediments may enable source identification and tracking of environmental processes. In this study we establish the distribution of mercury concentrations and mercury isotope ratios in surface sediments of three transects along the continental shelf and slope in Campos Basin-RJ-Brazil. The shelf showed on average lower total Hg concentrations (9.2 ± 5.3 ng g^{-1}) than the slope (24.6 ± 8.8 ng g^{-1}). MMHg average concentrations of shelf 0.15 ± 0.12 ng g^{-1} and slope 0.13 ± 0.06 ng g^{-1} were not significantly different. Distinct differences in Hg isotope ratio signatures were observed, suggesting that the two regions were impacted by different sources of Hg. The shelf showed more negative δ^{202}Hg and Δ^{199}Hg values ranging from −0.59 to −2.19‰ and from −0.76 to 0.08‰, respectively. In contrast, the slope exhibited δ^{202}Hg values from −0.29 to −1.82‰ and Δ^{199}Hg values from −0.23 to 0.09‰. Mercury found on the shelf, especially along the "D" and "I" transects, is depleted in heavy isotopes resulting in more negative δ^{202}Hg compared to the slope. Isotope ratios observed in the "D" and "I" shelf region are similar to Hg ratios commonly associated with plants and vegetation and very comparable to those detected in the estuary and adjoining mangrove forest, which suggests that Hg exported from rivers may be the dominating source of Hg in near coastal regions along the northern part of the shelf.

1. Introduction

Mercury (Hg) is a global pollutant due to its ability to undergo long-range transport from source regions to remote parts of the world, and its ubiquitous presence in aquatic ecosystems (Selin, 2009). Owing to its unique chemical and physical characteristics, mercury can undergo a variety of environmental reactions and processes, leading to a complex geochemical cycle. Much of the mercury originating from both anthropogenic and natural sources is eventually exported to the marine environment (Mason and Sheu, 2002). There, due to its affinity to particulate matter, mercury is readily scavenged from the water column and deposited to bottom sediments particularly in estuaries and coastal areas (Lamborg et al., 2016).

The global open oceans contribute about ~3.0 × 10^6 kg $year^{-1}$ of global Hg^0 emissions to the atmosphere (Driscoll et al., 2013). Hence, oceans become reservoirs in the global Hg cycle derived

* Corresponding author.
E-mail addresses: bfaraujo@yahoo.com.br (B.F. Araujo), crezende@uenf.br (C.E. Rezende).

http://dx.doi.org/10.1016/j.chemosphere.2017.03.056
0045-6535/

from various inputs of mercury. Although coastal areas are under considerably higher Hg stress, Hg export to the open ocean areas is not negligible (Amos et al., 2014). Direct atmospheric deposition is the primary source of Hg to the ocean whereas riverine discharge, mobilization from sediments, groundwater, and submarine hydrothermal inputs contribute lesser amounts (Mason et al., 2012). In support of this model, a recent detailed mass balance for the Mediterranean Sea showed that compared to terrestrial inputs twice as much Hg is deposited to the Sea directly from the atmosphere (Žagar et al., 2014).

In addition, the accumulation of Hg in the marine environment (e.g., sediments) is a potential risk because Hg can be easily converted into methylmercury (MMHg), which is neurotoxic and bioaccumulates in aquatic food webs (Fitzgerald et al., 2007). Mercury can become methylated by a number of biotic and abiotic means, with biological methylation likely dominating in the environment (Lamborg et al., 2006). Major sources of MMHg in the ocean are the production in sediments on the continental margin (Hammerschmidt and Fitzgerald, 2006), deep-sea deposits and hydrothermal vents and formation in oxic and low-oxygen regions of the water column, presumably through heterotrophic microbial activity (Lehnherr et al., 2011). However, questions remain unanswered regarding the relative significance of biotic and abiotic contributions of Hg to marine environments.

In this context, Hg isotope ratios are an effective tool for tracing sources and processes of Hg in the environment (Foucher et al., 2009). Fractionation of stable Hg isotopes has been demonstrated for geological (Smith et al., 2005), biological (Kritee et al., 2007) and photochemical (Bergquist and Blum, 2007) processes. Spatial and temporal variations in Hg isotope ratios in sediments have been measured in many studies to identify sources and to characterize processes (Das et al., 2013; Feng et al., 2010; Jackson et al., 2008; Foucher et al., 2009; Gehrke et al., 2009). Mercury has seven stable isotopes that increase in atomic mass from 196 to 204, with approximate isotopic abundances ranging from 0.15% (^{196}Hg) to 29.86% (^{202}Hg) (De Laeter et al., 2003).

The Campos Basin (CB) is the most important region of offshore petroleum production in Brazil. The region is also of ecological significance because upwelling events of the cold and nutrient rich South Atlantic Central Water (SACW) result in areas of high productivity in the water column (Campos et al., 2000). Hg is commonly associated with barite ($BaSO_4$) as a component of spent drilling mud that is discharged during drilling (Neff, 2002; Trefry and Smith, 2003; Pozebon et al., 2005). Trefry et al., 2007 showed considerably concentrations of Hg (48–558 ng g^{-1}) close to drilling sites in the Gulf of Mexico. Furthermore, the chemical composition of the discharged produced water is complex and highly variable, often containing dispersed oils and dissolved metals including Hg (Vegueria et al., 2002).

The Paraíba do Sul River (PSR) is the major freshwater supply to the South-eastern Brazilian coast, traversing three states (São Paulo, Minas Gerais and Rio de Janeiro) draining an area of approximately 57,300 km^2 with a length of 1500 km (Ovalle et al., 2013). It is proposed that the mean PSR sediment flux of 1.0–2.0 $\times$ 10^6 tons *per* year reaches the external continental shelf of Campos Basin (Lacerda et al., 2004). The PSR is impacted by deforestation of the margins leading to erosion, the use of agricultural pesticides, domestic sewage discharge and solid waste disposal, and the construction of numerous dams (Wanderley et al., 2014). Hg in the PSR basin may originate from two major sources: i) from Hg fungicides in sugar cane plantations until it was banned in the early 1980s and ii) from gold mining which uses Hg to amalgamate fine gold particles from river sediments (Lacerda et al., 1993; Araujo et al., 2015).

Campos Basin may be impacted by two main sources of mercury: i) exploration and production of oil and ii) Hg export from the Paraíba do Sul River (Araujo et al., 2010). Here, we conducted an investigation to establish the distribution of Hg concentrations and Hg isotopic composition in surface sediments of Campos Basin including the estuary region of the Paraíba do Sul River. Samples were collected along three transects (25–3000 m water depth) crossing the depositional profile, along the continental shield and slope of the studied marginal basin.

2. Material and methods

2.1. Study area

The Campos Basin, in the Southeastern Brazilian Continental Margin, extends from the Vitoria High (20°S) to the Cabo Frio High (24°S), covering an area of approximately 100,000 km^2 (Viana et al., 1998). The shelf has a mean width of 100 km and the continental slope is 40 km wide, and is characterized by a complex system of submarine channels and canyons. The shelf break varies from 80 m water depth in the northern area to 130 m water depth in the south with an average depth of 110 m. The average gradient of the slope is very gentle (2.5°), but both the upper (110–600 m) and the lower (1200–2000 m) slopes have steeper gradients. In the north (at approximately 1500 m water depth) the base of the slope is shallower than in the south (at approximately 2000 m) due to the occurrence of a submarine cone connected to the Almirante Camara submarine canyon (Viana et al., 1998). This basin is influenced by the Coastal Water, Brazil Current and South-Atlantic Central Water (Calado et al., 2010). The interaction between these three water masses, coupled to a complex circulation pattern marked by the meandering of the Brazil Current, are responsible for the sedimentation patterns in the shelf and slope region in Campos Basin (Mahiques et al., 2004). In deeper regions of the basin are observed the Antarctic Intermediate Water (550–1200 m depth) and the North-Atlantic Deep Water (NADW) (1500–3000 m depth) (Reid, 1989). The sedimentology of Campos Basin is heterogeneous composed of sand, shelf mud, carbonate banks and pelagic muds. Shelf muds derived from the discharge of the Paraiba do Sul river develop small mud ponds and large accumulations along the inner shelf about 150 km south of the river mouth (Viana et al., 1998).

2.2. Sampling

The study area is located in the Campos Basin in the state of Rio de Janeiro. Three transects of superficial sediments from 25 to 3000 m were sampled: A (located to the south and close to an upwelling area), D (located opposite the mouth of the Paraiba do Sul River) and I (located north near the top of Vitória-ES) (Fig. 1). We also collected superficial sediments (0–2 cm) from the estuary (six samples) and mangrove (five samples) of Paraíba do Sul river in 2008 and 2014, respectively (Fig. 1).

The sediment samples were collected from different Research Vessels (R/V) Gyre, Miss Emma McCall and/or Luke Thomas in 2009, as part of the Habitats Project – Campos Basin Environmental Heterogeneity and coordinated by CENPES/PETROBRAS. A box-corer was used to collect undisturbed 0–2 cm layers of the sediment. Sampling isobaths were 25, 50, 75, 100, 150, 400, 700, 1000, 1300, 1900, 2500 and 3000 m. The samples were stored at −20 °C, wet separated for their <2.0 mm fraction, freeze-dried (−50 °C for 72 h), ground and homogenized.

2.3. Geochemical measurements

The grain size was measured with a particle analyzer (Shimadzu SALD-310). Organic carbon (OC) was determined using a Flash 2000

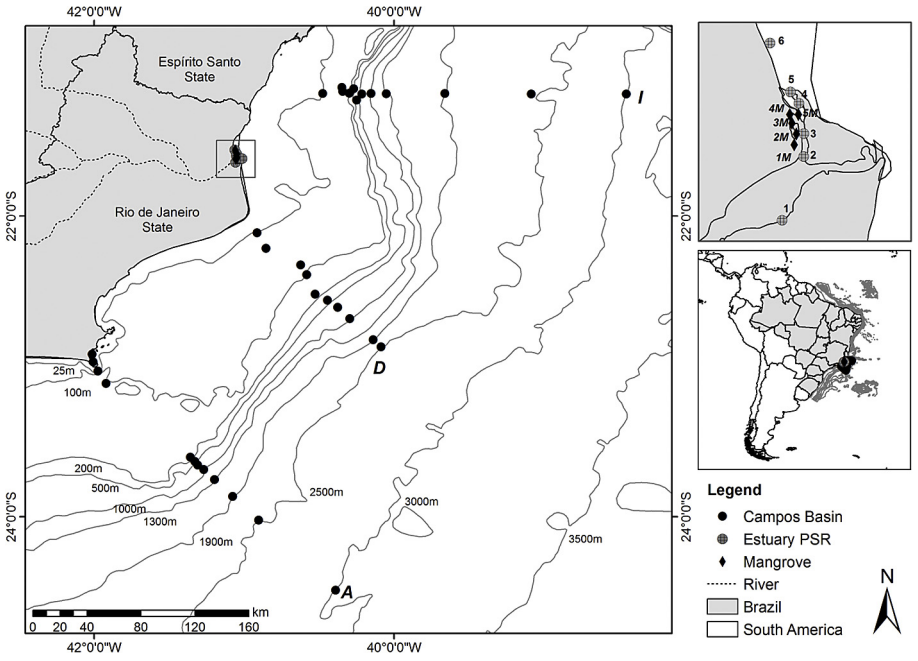

Fig. 1. Sampling stations of surface sediments (0–2 cm) collected from Campos Basin, the Paraíba do Sul river estuary and mangroves.

(Organic Elemental Analyzer – Thermo Scientific) elemental analyzer after removal of inorganic carbon with 1.0 M HCl (modified from Hedges and Stern, 1984). The total sulfur content (Total S) was determined based on the USEPA method 3052 (1996), after digestion in a microwave system model Mars Xpress (CEM) and measurement using an ICP-OES Varian Model 720 ES. These analysis were performed at the Laboratório de Ciências Ambientais at Universidade Estadual do Norte Fluminense – Campos dos Goytacazes – RJ- Brazil.

2.4. Total mercury (THg) and monomethylmercury (MMHg) analysis

To avoid contamination by Hg, all the materials and equipment was subjected to a rigorous cleaning protocol. Moreover, all unbagged equipment was handled with gloved hands in dedicated clean areas, including countertops covered by Teflon overlays within a Hg-free laminar flow-hood.

The THg and MMHg analysis were performed at Trent University Water Quality Centre (WQC). To determine the concentrations of total Hg (THg), samples of approximately 0.5 g (dry weight) were digested with a HNO_3:H_2SO_4 (7:3) mixture by gradually heating from 40 °C to 200 °C over a period of no less than 3 h. Acid digests were then cooled and diluted to 20 mL. Sample digests were analyzed for total mercury by cold-vapor atomic fluorescence spectrometry (CVAFS) using a Tekran 2600 system based on EPA Method 1631. Monomethylmercury (MMHg) was isolated by distillation, followed by GC/AFS measurement using a Tekran 2700 system based on EPA method 1630. THg and MMHg determinations of certified reference materials (NIST SRM, 1944 and IAEA-405) were within 90–110% and 80–95% of the certified valued, respectively, and coefficients of variation of triplicate analyses were <10%.

2.5. Mercury isotope ratio analysis

Hg isotope ratios were determined using a MC-ICP-MS instrument (Neptune, Thermo-Fisher, Germany) at the Trent University Water Quality Centre (WQC). Sample solutions (Hg concentrations varied from 0.5 to 2 ng/mL) were analyzed using a continuous flow cold vapor (CV) generation system after stannous chloride reduction (Foucher and Hintelmann, 2006). The Faraday cups were positioned to measure five Hg isotopes (^{198}Hg, ^{199}Hg, ^{200}Hg, ^{201}Hg, ^{202}Hg). Mass dependent fractionation (MDF) of Hg isotopes was expressed using the delta notation (δ^x Hg, in ‰):

$$\delta^{x}\mathrm{Hg}(‰) = \{(\delta^{x}\mathrm{Hg}/\delta^{198}\mathrm{Hg})_{\mathrm{sample}}/(\delta^{x}\mathrm{Hg}/\delta^{198}\mathrm{Hg})_{\mathrm{standard}}\text{-}1\} \times 1000 \quad (1)$$

where x = 199, 200, 201, 202 and “standard” represents the NIST SRM 3133 Hg solution. Mass independent fractionation (MIF) of both odd and even Hg isotopes was defined by the deviation from the theoretically predicted MDF and expressed as (in ‰):

$$\Delta^{199}\mathrm{Hg} = \delta^{199}\mathrm{Hg}\text{-}\ 0.252 \times \delta^{202}\mathrm{Hg} \quad (2)$$

$$\Delta^{200}\mathrm{Hg} = \delta^{200}\mathrm{Hg}\text{-}\ 0.502 \times \delta^{202}\mathrm{Hg} \quad (3)$$

$$\Delta^{201}\mathrm{Hg} = \delta^{201}\mathrm{Hg}\text{-}\ 0.752 \times \delta^{202}\mathrm{Hg} \quad (4)$$

Reproducibility of the isotopic data was assessed by measuring replicate sample digests once every 10 samples. We also analyzed an UM-Almadén Hg solution as secondary standard in addition to the bracketing standard NIST 3133. Our repeated measurements of UM-Almadén Hg gave long-term (n = 24) average δ^{202}Hg and Δ^{199}Hg values of −0.48 ± 0.16 and −0.02 ± 0.05‰, respectively, consistent with previously reported values (Blum and Bergquist, 2007).

2.6. Statistical analysis

Non-parametric statistic was conducted using the Mann-Whitney test to compare shelf and slope regions and *Spearman Correlation* was used to evaluate the relationship among variables. PERMANOVA multivariate analysis was performed to test the difference among the shelf, slope, mangrove and estuary.

3. Results

3.1. Geochemical parameters

The silt+clay, organic carbon (OC) and total sulfur (Total S) contents ranged from 0.05 to 95%, 0.07–1.43% and 0.01–0.18% for all transects, respectively (Table 1). The results showed that the superficial sediments consisted predominantly of silt-clay in the slope (400–3000 m). The OC content was higher in the "A" and "I" transects and the Total S average values were similar for all transects.

3.2. Total mercury and MMHg and mercury isotope composition in sediment

THg and MMHg average concentrations in transect "A" were 19.8 (3.3–33.2) ng g^{-1} and 0.18 (0.02–0.40) ng g^{-1}; in transect "D" 23.5 (3.3–51.6) ng g^{-1} and 0.11 (0.03–0.29) ng g^{-1}; and in transect "I" 26.1 (1.6–38.2) ng g^{-1} and 0.09 (0.02–0.16) ng g^{-1}, respectively (Fig. 2 and Table 3). The shelf showed lower THg average concentrations (9.2 ± 5.3 ng g^{-1}) than the slope (24.6 ± 8.8 ng g^{-1}). The MMHg average concentrations of shelf 0.15 ± 0.12 ng g^{-1} and slope 0.13 ± 0.06 ng g^{-1} were not significantly different (Mann-Whitney test, $p > 0.05$).

The THg and MMHg concentrations in mangrove sediments were significantly higher and varied from 45.8 to 152 (82.5 ± 49.4) ng g^{-1} and from 0.20 to 1.38 (0.79 ± 0.52) ng g^{-1}, respectively. The estuary showed THg concentration from 5.5 to 132 (54.1 ± 48.1) ng g^{-1} and MMHg values from 0.01 to 0.40 (0.10 ± 0.14) ng g^{-1} (Table 3). Contents of THg, Silt+clay and Total S content showed significant differences between shelf and slope regions (Mann-Whitney test). Significant spearman correlations were found between OC and THg (0.467, $p < 0.05$, $n = 33$), OC and MMHg (0.378, $p < 0.05$, $n = 33$) and silt+clay and OC (0.46, $n = 33$, $p < 0.05$).

The mercury isotope composition in the sediments is presented in Table 2. δ^{202}Hg and Δ^{199}Hg values vary from −0.32 to −2.19‰ (−0.96 ± 0.58‰) and −0.76 to 0.09‰ (−0.11 ± 0.12‰) for all transects, respectively (Table 3). No significant differences were observed among the three transects for δ^{202}Hg and Δ^{199}Hg. On the other hand, the delta values (MDF and MIF) between slope and shelf regions, especially for the "D" and "I" transect, are significantly different. Typically, the shelf region showed much more negative δ^{202}Hg values ranging from −0.59 to −2.19‰ (mean: −1.60 ± 0.56‰ n = 10) and Δ^{199}Hg values from - 0.76 to 0.08‰ (mean: −0.35 ± 0.30‰ n = 10) In contrast, the slope region exhibited δ^{202}Hg values from −0.29 to −1.82‰ (mean: −0.40 ± 0.50‰ n = 19) and Δ^{199}Hg from −0.23 to 0.09‰ (mean: −0.02 ± 0.08‰ n = 19). Table 2.

4. Discussion

4.1. Geochemical parameters

The silt+clay enrichment observed in the slope region is associated with the transport of fine material and low density over long distances, as described in other studies (Araujo et al., 2010; Souza et al., 2010; Wanderley et al., 2014). The transport of fine particles has been demonstrated to play an important role in delivering Hg to oceanic sediments and the organic carbon in these particles also has a strong ability to bind Hg (Yin et al., 2015). Thus, the significant correlation observed in our study between silt+clay and OC may indicate that this fraction facilitates the Hg transport to the Campos Basin.

It is important to note that sedimentation rates between shelf and slope differ greatly. According Godoy et al., 2006, the sedimentation rate in the slope region is approximately 1.7 cm K·$year^{-1}$ for the top 70 cm at locations of 2450 m depth. In other words, the top 2 cm would represent as much as 1200 years of sediment accumulation in the slope region. On the other hand, the Campos Basin shelf showed a sedimentation rate of approximately 550 cm K·$year^{-1}$ at locations with 79 m depth, with a gradual decrease in sedimentation rate towards the outer shelf (100 cm K·$year^{-1}$). Here, 2 cm of sediment would represent only 4–20 years of sediment deposition (Figueiredo et al., 2013). Hence, the Hg found in the slope region is presumably much older than Hg from the shelf.

4.2. Total Hg and MMHg

THg in the Campos Basin sediments was comparable to the background commonly found in ocean sediments around the world (20–100 ng g^{-1}) (Mason et al., 2012). Although the major source of mercury in the open ocean is from atmospheric deposition (Fitzgerald et al., 2007), we should consider the contribution from rivers, especially in near-shore regions as an estimated 90% of river-derived Hg is buried in sediments at ocean margins (Chester, 1990). Lacerda et al. (1993) described the influence of the Paraíba do Sul plume on the export of mercury to continental shelf sediments. Moreover, radioisotope studies suggest that the Paraíba do Sul plume can impact regions as far as 14–20 km offshore during the rainy season, with mixing rates of 2.6 kmd^{-1} that spread over a large area (Souza et al., 2010). It is therefore conceivable that mercury is also exported to the open ocean, mainly due to the effects of currents and hydrodynamic processes. In fact, Lamborg et al. (2014) reported that the North Atlantic Deep Water current, which occurs at about 1500–4000 m depth, is anomalously enriched in mercury relative to the deep waters of the South

Table 1
Silt-clay, organic carbon and total sulfur contents in surface sediments from Campos Basin.

	Depth (m)	A			D			I		
		Silt+clay (<63 μm) (%)	OC (%)	Total S (%)	Silt+Clay (<63 μm) (%)	OC (%)	Total S (%)	Silt+Clay (<63 μm) (%)	OC (%)	Total S (%)
Shelf	25	0.1	0.05	0.08	32.2	0.77	0.12	0.1	0.07	0.01
	50	1.94	0.15	0.03	0.1	0.08	0.03	29.8	0.76	0.1
	75	57.5	1.43	0.11	0.1	0.03	0.17			
	100	75.1	1.35	0.13				56.2	0.55	0.07
	150	22.9	0.72	0.1	50.3	0.5	0.13	36.9	0.59	0.08
Slope	400	57.8	0.57	0.07	72.8	0.6	0.1	91.9	1.4	0.17
	700	90.9	1.26	0.11	90.3	0.91	0.11	90.8	1.18	0.18
	1000	94.6	1.07	0.12				94.3	1.14	0.15
	1300	86.3	0.58	0.1	93.6	0.73	0.16	88.4	0.81	0.13
	1700	95.6	0.7	0.11	82.9	0.53	0.12	93.4	0.6	0.13
	2500	95.4	0.64	0.11	34.7	0.35	0.1	72.5	0.44	0.11
	3000	95.1	0.48	0.11	92	0.52	0.12	39.3	0.24	0.08

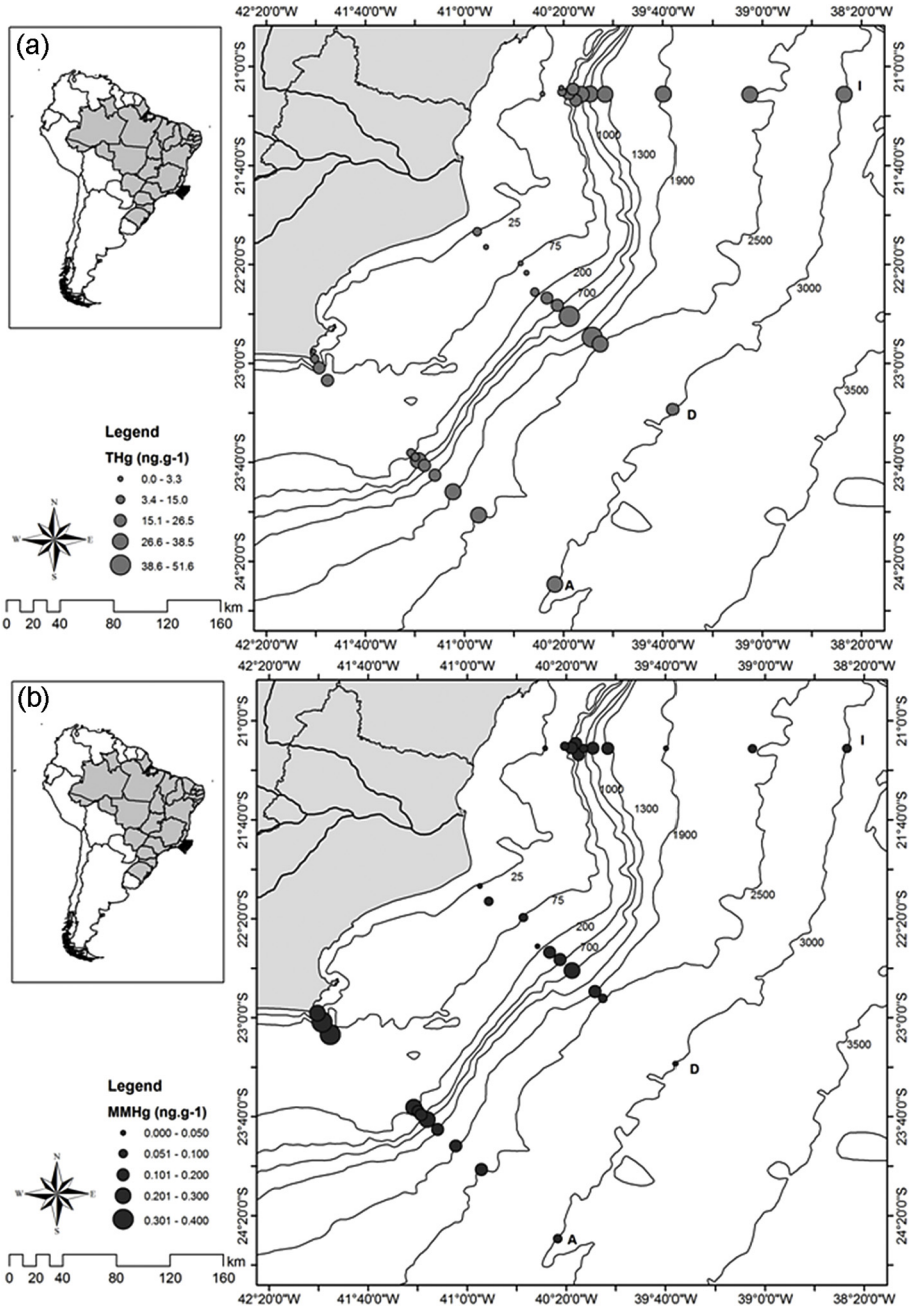

Fig. 2. THg (a) and MMHg (b) concentrations along three transects of Campos Basin.

Table 2
Comparison of THg and MMHg concentrations from this study with those measured in other marine settings.

Location	Total Hg (ng g^{-1})	MMHg (ng g^{-1})	Depth (m)	Comments	References
Campos Basin -Southeast Brazil	23.0 ± 12.4 (1.7–51.6)	0.13 ± 0.09 (<0.01–0.41)	25–3000	continental shelf and slope	This Study
mid-Atlantic continental shelf	0.62–69.4	0.08–0.96	16–819	continental shelf and slope	Hollweg et al., 2010
southern New England	6.7–34.1	0.01–0.31	59–131	continental shelf	Hammerschmidt and Fitzgerald, 2006
Northeast Gulf of Mexico	50 (31–67)	0.91 (0.2–1.9)	868	cold seep and background sites	Brown et al., 2013
Mediterranean Sea - Western and Eastern Basins	40.2–77.9	0.43–2.34	910–4063	Deep sea - slope	Ogrinc et al., 2007
Southern Baltic Sea	103 (5.8–225)	0.26 (0.06–0.94)	<100	Industrialized catchment area	Bełdowski et al., 2014

Table 3
Total mercury concentrations and mercury isotope ratios of sediments from Campos Basin, the Paraíba do Sul river estuary and mangroves.

	Depth	THg	MMHg	δ^{202}Hg	Δ^{199}Hg	Δ^{200}Hg	Δ^{201}Hg	THg	MMHg	δ^{202}Hg	Δ^{199}Hg	Δ^{200}Hg	Δ^{201}Hg	THg	MMHg	δ^{202}Hg	Δ^{199}Hg	Δ^{200}Hg	Δ^{201}Hg
	(m)	(ng g^{-1})	(ng g^{-1})	(‰)	(‰)	(‰)	(‰)	(ng g^{-1})	(ng g^{-1})	(‰)	(‰)	(‰)	(‰)	(ng g^{-1})	(ng g^{-1})	(‰)	(‰)	(‰)	(‰)
Transect A								D						I				Mangrove PSR	
Shelf	25	3.3	<0.01					13.3	0.05	−1.85	−0.41	−0.1	−0.32	1.7	0.02			45.8	0.2	−2	−0.42	0.04	−0.24
	50	8.3	0.22	−1.22	−0.10	−0.01	−0.16	3.3	0.07	−1.97	−0.17	0.08	−0.07	15	0.08	−1.61	−0.57	0	−0.47	152.1	0.75	−1.79	−0.67	−0.13	−0.37
	75	20	0.34	−1.1	−0.08	−0.02	−0.08	3.3	0.08	−2.19	−0.53	−0.15	−0.48							40.1	0.38	−2.1	−0.58	−0.31	−0.54
	100	18.3	0.41	−0.59	0.08	0.01	−0.09							19.9	0.14	−1.89	−0.76	0.01	−0.54	57.7	1.26	−1.74	−0.42	0.14	−0.34
	150	13.9	0.22					11.7	0.04	−1.40	−0.11	0.06	−0.09	22.2	0.12	−1.92	−0.59	−0,04	0.46	116.7	1.38	−1.79	−0.55	0.11	−0.61
Slope	400	11.6	0.18					23.3	0.16	−1.03	0.06	0.04	−0.14	23.3	0.16	−1.82	−0.23	−0.12	−0.07	Estuary PSR					
	700	18.3	0.12	−0.73	−0.07	−0.06	0.14	26.6	0.17	−0.8	0.05	0	−0.1	34.9	0.08	−1.24	−0.11	−0.01	−0.21	39.5	0.01	−1.93	−0.53	0.05	−0.47
	1000	26.6	0.2	−0.34	0.03	0	0.07	51.6	0.29	−0.96	−0.09	−0.05	0.14	35	0.13	−0.55	−0.13	−0.07	−0.28	7.5	0.02	−1.62	−0.82	−0.01	−0.51
	1300	26.3	0.14	−0.52	0.01	−0.02	0.05							33.3	0.13	−0.49	0	0.01	−0.07	132.5	0.4	−2.07	−0.58	−0.02	−0.53
	1900	28.2	0.12	−0.39	0.06	0.03	−0.08	48.2	0.16	−0.74	0	0.01	0.08	38.2	0.04	−0.71	−0.03	0.03	0	5.5	0.01	−1.99	−0.56	−0.04	−0.51
	2500	30	0.16	−0.4	0.09	0.07	−0.14	31.6	0.05	−1.15	0.01	0.02	−0.01	31.6	0.06	−0.56	0	0.02	0	60	0.11	−1.85	−0.57	−0.03	−0.49
	3000	33.3	0.07	−0.32	0.07	0.06	−0.17	21.6	0.03	−0.63	−0.02	0	0	31.6	0.07	−0.43	−0.07	−0.01	−0.01	79.8	0.1	−1.98	−0.51	−0.11	−0.16

Atlantic, Southern and Pacific oceans, probably as a result of the incorporation of anthropogenic mercury. Zhang et al. (2014) and Lamborg et al. (2014) suggested that the deep North Atlantic is a notable location of current pollution Hg storage (approx. 25% of total). Sunderland and Mason (2007) noted that in addition to atmospheric deposition, regional-scale variability in air sea exchange of mercury, particulate settling, and lateral and vertical seawater flow are all important for determining the direction and rate of mercury concentrations in the open ocean.

MMHg represents less than 1% of the THg in all transects. Only in the "A" transect was MMHg higher in the upper slope (400–1900 m) compared to the shelf region. The "A" transect is located in an upwelling area and is characterized by high productivity and organic matter availability, which may contribute to higher methylation rates. The Hg methylation is affected by the bioavailability of Hg(II) and by the activity of Hg-methylating microbes, both of which are significantly influenced by biogeochemical changes across salinity and productivity gradients (Hollweg et al., 2010). Upwelling zones have been related with Hg supply to ocean surface waters (Cossa et al., 2004; Soerensen et al., 2010; Figueiredo et al., 2013). Furthermore, upwelling regions have been of the great importance to Hg biogeochemical cycle due to the high productivity and large organic matter deposition in these areas (Silva et al., 2011). Indeed, Figueiredo et al. (2013) found a relationship between mercury and organic carbon in shelf sediments in the south of Campos Basin, suggesting that upwelling processes and primary production may play a role in controlling Hg distribution and deposition along the continental shelf.

The "D" transect, is closest to the Paraíba do Sul river. Although its drainage basin was affected by human influence such as gold mining and use of organo-mercurial fungicides in sugar cane plantations in the 80s (Lacerda et al., 1993), no significant differences in THg and MMHg concentrations were observed relative to others transects.

Significant correlations between OC and THg, OC and MMHg and Silt+Clay and THg were observed in this study. However, in addition to carbon, other processes such as adsorption on Fe and Mn oxyhydroxides may also play an effective role in the sequestration of Hg (Gagnon et al., 1997). Lamborg et al. (2016) also suggested that also calcium carbonate may also influence the sorption of Hg. Phases such as biogenic silica and lithogenic material, however, are considered unimportant. Overall, Hg scavenging and associated particle cycling is likely region and time-dependent as the dominant materials in marine particles change as a result of local biogeochemistry and ecosystem structure. In addition, Das et al. (2013) found a strong correlation between Hg and other metals concentration in salt marsh sediments (e.g. Fe, Co, Pb, Cu, Zn, Nd, and Th) with correlation coefficients between 0.72 and 0.83, which were all related to sediment size distribution. In comparison, MMHg concentrations in Campos Basin are lower than in coastal polluted sediment from the Mediterranean Sea, where MMHg concentrations vary from 0.43 to 2.34 ng g^{-1} (Ogrinc et al., 2007) and likely originate from the Adriatic Sea, which is influenced by several and very significant anthropogenic sources of Hg. The MMHg concentrations from Campos Basin were similar to other oceanic areas such as the Mid-Atlantic shelf (Hollweg et al., 2010) and the continental shelf of southern New England (Hammerschmidt and Fitzgerald, 2006) (Table 2).

In relation to the THg and MMHg in estuary and mangrove areas, Araujo et al. (2015) found higher mercury availability in the fluvial and estuarine areas compared to mangroves in PRS and emphasized the importance of mangrove ecosystems to act as a geochemical barrier for Hg and that the continuous reduction of the Paraíba do Sul river mangrove forest could result in increased transport of Hg to the ocean.

4.3. Isotope ratios of mercury

Generally speaking, two main factors may affect Hg isotope ratios in environmental samples and must be considered when interpreting differences in Hg isotope composition: Hg isotope fractionation during geochemical cycling and the mixing of Hg from different sources with distinct isotope signatures (Yin et al., 2015). According to Blum et al. (2014), marine sediments that were deposited before modern increases in anthropogenic Hg emissions (i.e. pre-1850), often display limited MIF (Δ^{199}Hg = 0.00 ± 0.13‰, n = 51) and a moderate range in δ^{202}Hg values (mean = −1.00 ± 0.48‰, n = 51). Younger marine sediments that were influenced by anthropogenic sources, but not directly associated with a point source of Hg contamination, may have similar but more variable Δ^{199}Hg (mean = 0.03 ± 0.13‰, n = 191) and δ^{202}Hg values (mean = −0.91 ± 0.64‰, n = 191). In comparison, δ^{202}Hg values in the slope region of Campos Basin are comparable to values found in other oceanic regions, despite the fact, these areas do not have the similar physiography, sedimentation control and regime of currents. Similar δ^{202}Hg averages were observed for pre-anthropogenic Mediterranean background (−0.76‰ ± 0.16‰) and sapropel samples (−0.91‰ ± 0.15‰) (Gehrke et al., 2009). Moreover, Mil-Homens et al., 2013 found an average of −0.59‰ ± 0.04‰ in sediments from the central Portuguese Margin at 2084 m water depth.

Most striking were the observed differences in Hg isotope composition between sediments from the shelf and slope ($p < 0.05$) as illustrated in Fig. 3. Hg found on the shelf, especially along the "D" and "I" transects, is depleted in heavy isotopes resulting in more negative δ^{202}Hg compared to the slope. Values are very comparable to those detected in the estuary and adjoining mangrove forest, which suggests that the shelf Hg may be exported from rivers and is the dominating source of Hg in near coastal regions along the northern part of the shelf. The "D" transect in particular is directly influenced by the Paraíba do Sul River. On the other hand, the "I" transect is influenced by smaller rivers (Anchieta, Itapemirin, Itabapoana), streams and coastal lagoons, which all have similar regional geochemistry. The "I" transect was the most variable. It appears that the riverine export of Hg extended beyond the shelf into the upper slope, where more negative δ^{202}Hg values were observed down to 700 m water depth. A multivariate PERMANOVA analysis, confirmed significant differences in δ^{202}Hg between slope and shelf, estuary and mangrove ($P < 0.005$) (Table 4). This interpretation is consistent with recent studies, which collectively converge on a δ^{202}Hg signature of approximately −2.0‰ for vegetation and soils, at least for Europe

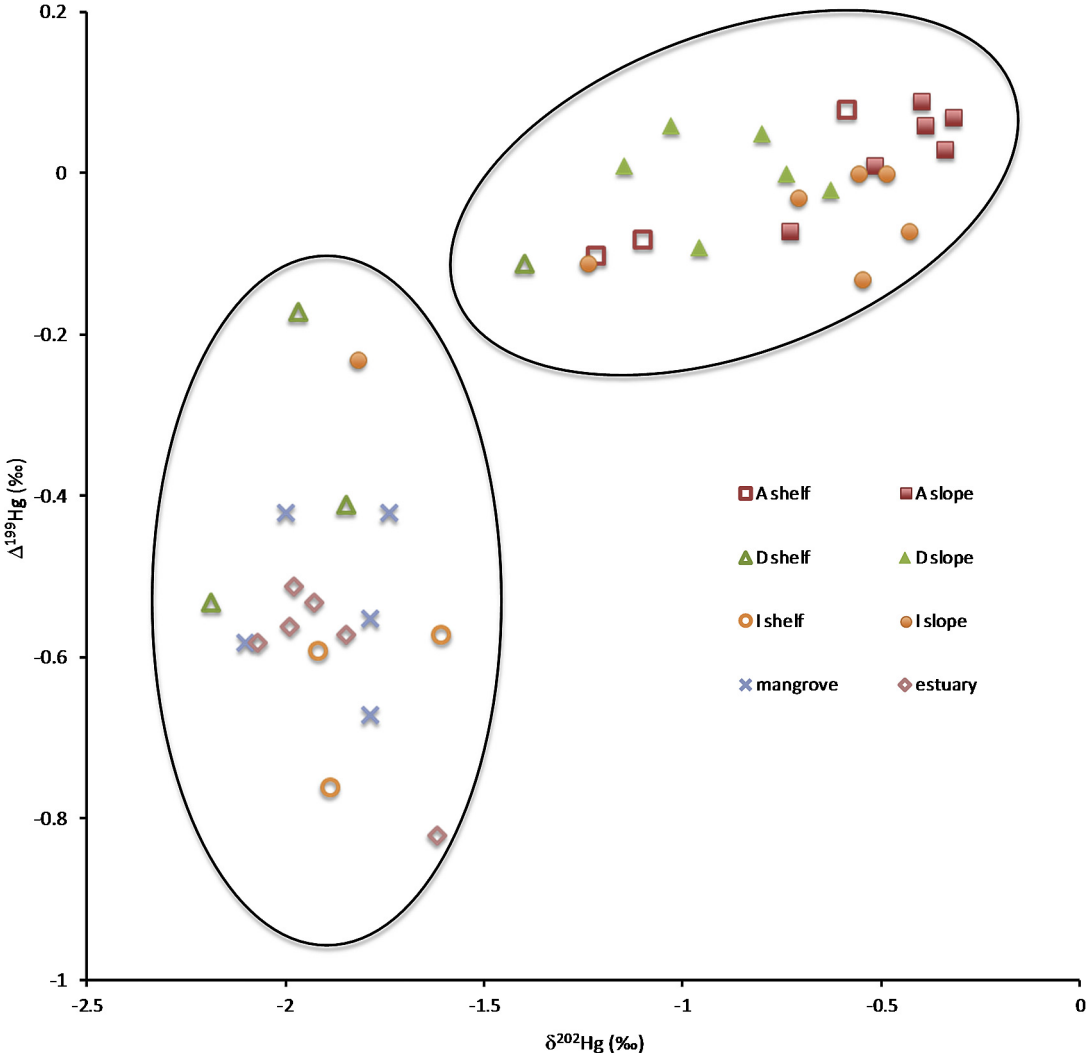

Fig. 3. Relationship between Δ^{199}Hg and δ^{202}Hg in sediment samples from Campos Basin, mangroves and the RPS estuary.

Table 4
PERMANOVA of spatial Hg distribution on shelf, slope, mangrove and estuary of Campos Basin.

Factors	MS	Pseudo-*F*	p
Spatial	22.757	25.601	0.0001*
Pairwise tests			
Groups		*t*	p
Shelf, Slope		5.0617	0.0001*
Shelf, Mangrove		1.3065	0.2144
Shelf, Estuary		1.5867	0.131
Slope, Mangrove		7.8556	0.0001*
Slope, Estuary		8.7943	0.0001*
Mangrove, Estuary		0.3160	0.8209

(Enrico et al., 2016; Jiskra et al., 2015). If also true for South America, the significantly more negative δ^{202}Hg in the shelf region near transect "D" and "I" could indeed indicate the export of terrestrial Hg through the PSR and other smaller rivers. However, the current dataset does not allow a differentiation between Hg associated with distinct anthropogenic sources (e.g. gold mining or Hg fungicides) or Hg fractionation as result of terrestrial Hg processes, which generate naturally more negative δ^{202}Hg.Interestingly, Hg in the shelf region along the "A" transect shows more positive values, which suggest that this area is less influences by exports from rivers or that other geochemical processes are dominant. It is noteworthy, that there is a steep drop near the coast in the "A" transect, which may prevent exported Hg loaded particles to settle near shore, explaining the mixed character of Hg at this location. Furthermore, the shelf in the southern region of the Campos Basin is wider (approximately 120 km) compared to the northern area (approximately 42 km) affecting the deposition of transported material along the shelf.

Most sampling stations in the Campos Basin slope showed near zero or slightly positive MIF (Δ^{199}Hg) (Table 3). Other marine sediments are also characterized by positive Δ^{199}Hg values, including the Central Portuguese Margin (+0.09 ± 0.04‰) (Mil-Homens et al., 2013), mid-Pleistocene sapropels from the Mediterranean Sea (+0.11 ± 0.03‰) (Gehrke et al., 2009) and pre-mining sediments in the San Francisco Bay region (+0.17 ± 0.03‰) (Donovan et al., 2013). One possible explanation for positive Δ^{199}Hg values in oceanic sediments could be Hg associated with atmospheric deposition, which represents a significant source in the biogeochemical cycle of Hg in oceans (Fu et al., 2010), and is frequently characterized by positive Δ^{199}Hg (Chen et al., 2012; Enrico et al., 2016; Sherman et al., 2012). In addition, we cannot exclude that post-depositional MIF processes may also alter the Δ^{199}Hg values. The observed positive Δ^{199}Hg data are broadly consistent with Hg as a product of photoreduction (Sonke, 2011; Das et al., 2013).

As with the δ^{202}Hg along the "D" and "I" transects, MIF is also distinctly different in the shelf region compared to the slope. Values for Δ^{199}Hg on the shelf are much more negative and similar to Δ^{199}Hg found in the estuary and mangrove forest, supporting the idea that Hg is exported from rivers and that the Hg is fractionated as a result of processes or sources originating in riverine settings. For example, negative Δ^{199}Hg values were previously reported for lichens and other plant samples (e.g. Carignan et al., 2009). Differences between slope and shelf were much less pronounced in transect "A", with Δ^{199}Hg values being indistinguishable between slope and shelf along this transect. This area is also influenced by upwelling phenomena that could influence Hg processes. The presence of meanders, cyclonic and anticyclonic eddies in the middle portion of the southern continental shelf can create upward and downward movements as well as lateral transport of water masses (Mahiques et al., 2004). Thus, the type and amount of material transported to the seafloor are associated with the oceanographic forcing in the region and can influence the Hg deposition in this part of the Basin (Figueiredo et al., 2013).

Acknowledgments

The authors thank PETROBRAS for providing samples and supporting the chemical analyses. B.F. Araujo acknowledges a PhD's fellowship from CAPES and FAPERJ. The authors are also grateful to the *Laboratório de Ciências Ambientais* of the *Centro de Biociências e Biotecnologia* at the *Universidade Estadual do Norte Fluminense* for the use of its infrastructure. Thanks are also extended to INCT-TMCOcean on the Continent-Ocean Materials Transfer (CNPq: 573.601/08-9). C.E. Rezende received financial support from CNPq (506.750/2013-2) and FAPERJ (E-26/110.032/2011).

References

Amos, H.M., Jacob, D.J., Kocman, D., Horowitz, H.M., Zhang, Y., Dutkiewicz, S., Horvat, M., Corbitt, E.S., Krabbenhoft, D.P., Sunderland, E.M., 2014. Global biogeochemical implications of mercury discharges from rivers and sediment burial. Environ. Sci. Technol. 48 (16), 9514–9522.
Araujo, B.F., Almeida, M.G., Salomão, M.S.M.B., Gobo, R.R., Siqueira, V.C., Ovalle, A.R.C., Rezende, C.E., 2010. Distribuição de Hg total e suas associações com diferentes suportes geoquímicos em sedimentos marinhos da margem continental Brasileira: bacia de Campos–Rio de Janeiro. Quím. Nova 33 (3), 501–507.
Araujo, B.F., de Almeida, M.G., Rangel, T.P., de Rezende, C.E., 2015. Distribuição e fracionamento do Hg em sedimentos do rio Paraíba do Sul –RJ Brasil. Quím. Nova 38 (1), 30–36.
Bergquist, B.A., Blum, J.D., 2007. Mass-dependent and-independent fractionation of Hg isotopes by photoreduction in aquatic systems. Science 318 (5849), 417–420.
Bełdowski, J., Miotk, M., Bełdowska, M., Pempkowiak, J., 2014. Total, methyl and organic mercury in sediments of the Southern Baltic Sea. Mar. Pollut. Bull. 87 (1), 388–395.
Blum, J.D., Bergquist, B.A., 2007. Reporting of variations in the natural isotopic composition of mercury. Anal. Bioanal. Chem. 388 (2), 353–359.
Blum, J.D., Sherman, L.S., Johnson, M.W., 2014. Mercury isotopes in earth and environmental sciences. Annu. Rev. Earth Planet. Sci. 42, 249–269.
Brown, G., Sleeper, K., Johnson, M.W., Blum, J.D., Cizdziel, J.V., 2013. Mercury concentrations, speciation, and isotopic composition in sediment from a cold seep in the northern Gulf of Mexico. Mar. Pollut. Bull. 77 (1), 308–314.
Calado, L., da Silveira, I.C.A., Gangopadhyay, A., de Castro, B.M., 2010. Eddy-induced upwelling off Cape São Tome' (22 S, Brazil). Cont. Shelf Res. 30 (10–11), 1181–1188.
Campos, E.J., Velhote, D., da Silveira, I.C., 2000. Shelf break upwelling driven by Brazil Current cyclonic meanders. Geophys. Res. Lett. 27 (6), 751–754.
Carignan, J., Estrade, N., Sonke, J.E., Donard, O.F., 2009. Odd isotope deficits in atmospheric Hg measured in lichens. Environ. Sci. Technol. 43 (15), 5660–5664.
Chen, J., Hintelmann, H., Feng, X., Dimock, B., 2012. Unusual fractionation of both odd and even mercury isotopes in precipitation from Peterborough, ON, Canada. Geochim. Cosmochim. Acta 90, 33–46.
Chester, R., 1990. The transport of material to the oceans: relative flux magnitudes. In: Marine Geochemistry. Springer Netherlands, pp. 149–191.
Cossa, D., Cotté-Krief, M.H., Mason, R.P., Bretaudeau-Sanjuan, J., 2004. Total mercury in the water column near the shelf edge of the European continental margin. Mar. Chem. 90 (1), 21–29.
Das, R., Bizimis, M., Wilson, A.M., 2013. Tracing mercury seawater vs. atmospheric inputs in a pristine SE USA salt marsh system: mercury isotope evidence. Chem. Geol. 336, 50–61.
Donovan, P.M., Blum, J.D., Yee, D., Gehrke, G.E., Singer, M.B., 2013. An isotopic record of mercury in San Francisco Bay sediment. Chem. Geol. 349, 87–98.
Driscoll, C.T., Mason, R.P., Chan, H.M., Jacob, D.J., Pirrone, N., 2013. Mercury as a global pollutant: sources, pathways, and effects. Environ. Sci. Technol. 47 (10), 4967–4983.
EPA Method 3052, 1996. Microwave assisted acid digestion of siliceous and organically based matrices. In: Test Methods for Evaluating Solid Waste, 3rd Edition. US Environmental Protection Agency, Washington DC. 3rd Update.
Enrico, M., Roux, G.L., Marusczak, N., Heimbürger, L.E., Claustres, A., Fu, X., Sun, R., Sonke, J.E., 2016. Atmospheric mercury transfer to peat bogs dominated by gaseous elemental mercury dry deposition. Environ. Sci. Technol. 50 (5), 2405–2412.
Feng, X., Foucher, D., Hintelmann, H., Yan, H., He, T., Qiu, G., 2010. Tracing mercury contamination sources in sediments using mercury isotope compositions. Environ. Sci. Technol. 44 (9), 3363–3368.
Figueiredo, T.S., Albuquerque, A.L.S., Sanders, C.J., Cordeiro, L.G., Silva-Filho, E.V., 2013. Mercury deposition during the previous century in an upwelling region; Cabo Frio, Brazil. Mar. Pollut. Bull. 76 (1), 389–393.

Fitzgerald, W.F., Lamborg, C.H., Hammerschmidt, C.R., 2007. Marine biogeochemical cycling of mercury. Chem. Rev. 107 (2), 641–662.
Foucher, D., Hintelmann, H., 2006. High-precision measurement of mercury isotope ratios in sediments using cold-vapor generation multi-collector inductively coupled plasma mass spectrometry. Anal. Bioanal. Chem. 384 (7–8), 1470–1478.
Foucher, D., Ogrinc, N., Hintelmann, H., 2009. Tracing mercury contamination from the Idrija mining region (Slovenia) to the Gulf of Trieste using Hg isotope ratio measurements. Environ. Sci. Technol. 43 (1), 33–39.
Fu, X., Feng, X., Zhang, G., Xu, W., Li, X., Yao, H., Liu, N., 2010. Mercury in the marine boundary layer and seawater of the South China Sea: concentrations, sea/air flux, and implication for land outflow. J. Geophys. Res. Atmos. (1984–2012) 115, D6.
Gagnon, C., Pelletier, É., Mucci, A., 1997. Behaviour of anthropogenic mercury in coastal marine sediments. Mar. Chem. 59 (1), 159–176.
Gehrke, G.E., Blum, J.D., Meyers, P.A., 2009. The geochemical behavior and isotopic composition of Hg in a mid-Pleistocene western Mediterranean sapropel. Geochim. Cosmochim. Acta 73 (6), 1651–1665.
Godoy, M.L.D., Godoy, J.M., Kowsmann, R., Dos Santos, G.M., Da Cruz, R.P., 2006. 234 U and 230 Th determination by FIA-ICP-MS and application to uranium-series disequilibrium in marine samples. J. Environ. Radioact. 88 (2), 109–117.
Hammerschmidt, C.R., Fitzgerald, W.F., 2006. Methylmercury in freshwater fish linked to atmospheric mercury deposition. Environ. Sci. Technol. 40 (24), 7764–7770.
Hedges, J.I., Stern, J.H., 1984. Carbon and nitrogen determinations of carbonate-containing solids. Limnol. Oceanogr. 29 (3), 657–663.
Hollweg, T.A., Gilmour, C., Mason, R.P., 2010. Mercury and methylmercury cycling in sediments of the mid-Atlantic continental shelf and slope. Limnol. Oceanogr. 55 (6), 2703–2722.
Jackson, T.A., Whittle, D.M., Evans, M.S., Muir, D.C., 2008. Evidence for mass-independent and mass-dependent fractionation of the stable isotopes of mercury by natural processes in aquatic ecosystems. Appl. Geochem. 23 (3), 547–571.
Jiskra, M., Wiederhold, J.G., Skyllberg, U., Kronberg, R.M., Hajdas, I., Kretzschmar, R., 2015. Mercury deposition and re-emission pathways in boreal forest soils investigated with Hg isotope signal. Environ. Sci. Technol. 49, 7188–7196.
Kritee, K., Blum, J.D., Johnson, M.W., Bergquist, B.A., Barkay, T., 2007. Mercury stable isotope fractionation during reduction of Hg (II) to Hg (0) by mercury resistant microorganisms. Environ. Sci. Technol. 41 (6), 1889–1895.
Lacerda, L.D., Carvalho, C.E.V., Rezende, C.E., Pfeiffer, W.C., 1993. Mercury in sediments from the Paraíba do Sul River continental shelf, SE Brazil. Mar. Pollut. Bull. 26 (4), 220–222.
Lacerda, L.D., Rezende, C.E., Ovalle, Á.R., Carvalho, C.E.V., 2004. Mercury distribution in continental shelf sediments from two offshore oil fields in southeastern Brazil. Bull. Environ. Contam. Toxicol. 72 (1), 178–185.
De Laeter, J.R., Böhlke, J.K., De Bièvre, P., Hidaka, H., Peiser, H.S., Rosman, K.J.R., Taylor, P.D.P., 2003. Atomic weights of the elements: review 2000 (IUPAC Technical Report). Pure Appl. Chem. 75, 683–800.
Lamborg, C.H., Von Damm, K.L., Fitzgerald, W.F., Hammerschmidt, C.R., Zierenberg, R., 2006. Mercury and monomethylmercury in fluids from Sea Cliff submarine hydrothermal field, Gorda Ridge. Geophys. Res. Lett. 33 (17), L17606. http://dx.doi.org/10.1029/2006GL026321.
Lamborg, C.H., Hammerschmidt, C.R., Bowman, K.L., Swarr, G.J., Munson, K.M., Ohnemus, D.C., Lam, P.J., Heimburger, L., Rijkenberg, M.J.A., Saito, M.A., 2014. A global ocean inventory of anthropogenic mercury based on water column measurements. Nature 512 (7512), 65–68.
Lamborg, C.H., Hammerschmidt, C.R., Bowman, K.L., 2016. An examination of the role of particles in oceanic mercury cycling. Philos. Trans. R. Soc. A 374 (2081), 20150297.
Lehnherr, I., Louis, V.L.S., Hintelmann, H., Kirk, J.L., 2011. Methylation of inorganic mercury in polar marine waters. Nat. Geosci. 4 (5), 298–302.
Mahiques, M.M., Tessler, M.G., Maria Ciotti, A., da Silveira, I.C.A., Sousa, S.H.M.E., Figueira, R.C.L., Tassinari, C.C.G., Furtado, V.V., Passos, R.F., 2004. Hydrodynamically driven patterns of recent sedimentation in the shelf and upper slope off Southeast Brazil. Cont. Shelf Res. 24 (15), 1685–1697.
Mason, R.P., Sheu, G.R., 2002. Role of the ocean in the global mercury cycle. Glob. Biogeochem. Cycles 16.
Mason, R.P., Choi, A.L., Fitzgerald, W.F., Hammerschmidt, C.R., Lamborg, C.H., Soerensen, A.L., Sunderland, E.M., 2012. Mercury biogeochemical cycling in the ocean and policy implications. Environ. Res. 119, 101–117.
Mil-Homens, M., Blum, J., Canario, J., Caetano, M., Costa, A.M., Lebreiro, S.M., Trancoso, M., Richter, T., de Stigter, H., Johnson, M., Branco, V., Cesario, R., Mouro, F., Mateus, M., Boer, W., Melo, Z., 2013. Tracing anthropogenic Hg and Pb input using stable Hg and Pb isotope ratios in sediments of the central Portuguese Margin. Chem. Geol. 336, 62–71.
Neff, J.M., 2002. Fates and Effects of Mercury from Oil and Gas Exploration and Production Operations in the Marine Environment. Prepared under contract for American Petroleum Institute and the Ad Hoc Upstream Industry Mercury Working Group.
Ogrinc, N., Monperrus, M., Kotnik, J., Fajon, V., Vidimova, K., Amouroux, D., Kocman, D., Tessier, E., Žižek, S., Horvat, M., 2007. Stribution of mercury and methylmercury in deep-sea surficial sediments of the Mediterranean Sea. Mar. Chem. 107 (1), 31–48.
Ovalle, A.R.C., Silva, C.F., Rezende, C.E., Gatts, C.E.N., Suzuki, M.S., Figueiredo, R.O., 2013. Long-term trends in hydrochemistry in the Paraíba do Sul River, southeastern Brazil. J. Hydrol. 481, 191–203.
Pozebon, D., Lima, E.C., Maia, S.M., Fachel, J.M., 2005. Heavy metals contribution of non-aqueous fluids used in offshore oil drilling. Fuel 84 (1), 53–61.
Reid, J.L., 1989. On the total geostrophic circulation of the South Atlantic Ocean: flow patterns, tracers, and transports. Prog. Oceanogr. 23, 149–244.
Selin, N.E., 2009. Global biogeochemical cycling of mercury: a review. Annu. Rev. Environ. Resour. 34 (1), 43.
Sherman, L.S., Blum, J.D., Douglas, T.A., Steffen, A., 2012. Frost flowers growing in the Arctic ocean-atmosphere–sea ice–snow interface: 2. Mercury exchange between the atmosphere, snow, and frost flowers. J. Geophys. Res. Atmos. 117, D14.
Silva, C.A.D., Tessier, E., Kütter, V.T., Wasserman, J.C., Donard, O.F., Silva-Filho, E.V., 2011. Mercury speciation in fish of the Cabo Frio upwelling region, SE-Brazil. Brazilian Journal of Oceanography 59 (3), 259–266.
Smith, C.N., Kesler, S.E., Klaue, B., Blum, J.D., 2005. Mercury isotope fractionation in fossil hydrothermal systems. Geology 33 (10), 825–828.
Soerensen, A.L., Sunderland, E.M., Holmes, C.D., Jacob, D.J., Yantosca, R.M., Skov, H., Mason, R.P., 2010. An improved global model for air-sea exchange of mercury: high concentrations over the North Atlantic. Environ. Sci. Technol. 44 (22), 8574–8580.
Sonke, J.E., 2011. A global model of mass independent mercury stable isotope fractionation. Geochim. Cosmochim. Acta 75 (16), 4577–4590.
Souza, T.A., Godoy, J.M., Godoy, M.L.D., Moreira, I., Carvalho, Z.L., Salomão, M.S.M., Rezende, C.E., 2010. Use of multitracers for the study of water mixing in the Paraíba do Sul River estuary. J. Environ. Radioact. 101 (7), 564–570.
Sunderland, E.M., Mason, R.P., 2007. Human impacts on open ocean mercury concentrations. Global Biogeochemical Cycles 21 (4).
Trefry, J.H., Smith, J.P., 2003. Forms of mercury in drilling fluid barite and their fate in the marine environment. A review and synthesis. In: SPE 80571. SPE/EPA/DOE Exploration and Production Environmental Conference. Society of Petroleum Engineers, San Antonio, TX. Richardson (TX), pp. 1–10.
Trefry, J.H., Trocine, R.P., McElvaine, M.L., Rember, R.D., Hawkins, L.T., 2007. Total mercury and methylmercury in sediments near offshore drilling sites in the Gulf of Mexico. Environ. Geol. 53 (2), 375–385.
U.S. EPA. Method 1631, 1999. Mercury in Water by Oxidation, Purge and Trap, and Cold Vapor Atomic Fluorescence Spectrometry. Washington (DC)7 Office of Water, Engineering and Analysis Division (4303); U.S. EPA 821-R-95–027.
Vegueria, J.S.F., Godoy, J.M., Miekeley, N., 2002. Environmental impact in sediments and seawater due to discharges of Ba, 226 Ra, 228 Ra, V, Ni and Pb by produced water from the Bacia de Campos oil field offshore platforms. Environ. Forensics 3 (2), 115–123.
Viana, A.R., Faugeres, J.C., Kowsmann, R.O., Lima, J.A.M., Caddah, L.F.G., Rizzo, J.G., 1998. Hydrology, morphology and sedimentology of the Campos continental margin, offshore Brazil. Sediment. Geol. 115 (1–4), 133–157.
Wanderley, C.V., Godoy, J.M., Godoy, M.L.D., Rezende, C.E., Lacerda, L.D., Moreira, I., Carvalho, Z.L., 2014. Evaluating sedimentation rates in the estuary and shelf region of the Paraíba do Sul River, Southeastern Brazil. J. Braz. Chem. Soc. 25 (1), 50–64.
Yin, R., Feng, X., Chen, B., Zhang, J., Wang, W., Li, X., 2015. Identifying the sources and processes of mercury in subtropical estuarine and ocean sediments using Hg isotopic composition. Environ. Sci. Technol. 49 (3), 1347–1355.
Žagar, D., Sirnik, N., Četina, M., Horvat, M., Kotnik, J., Ogrinc, N., Hedgecock, I.M., Cinnirella, S., De Simone, F., Gencarelli, Christian N., Pirrone, N., 2014. Mercury in the Mediterranean, Part 2: processes and mass balance. Environ. Sci. Pollut. Res. 21 (6), 4081–4094.
Zhang, Y., Jaeglé, L., Thompson, L., 2014. Natural biogeochemical cycle of mercury in a global three-dimensional ocean tracer model. Glob. Biogeochem. Cycles 28 (5), 553–570.